Electronic structure and ferroelectricity in $SrBi_2Ta_2O_9$

M. G. Stachiotti
Instituto de Física Rosario, Universidad Nacional de Rosario, 27 de Febrero 210 Bis, 2000 Rosario, Argentina

C. O. Rodriguez
IFLYSIB, Grupo de Física del Sólido, CC 565, La Plata 1900, Argentina

C. Ambrosch-Draxl
Institut für Theoretische Physik, Universität Graz, Universitätsplatz 5, A-8010 Graz, Austria

N. E. Christensen
Institute of Physics and Astronomy, Aarhus University, DK-8000 Aarhus C, Denmark
(Received 22 December 1999)

The electronic structure of $SrBi_2Ta_2O_9$ is investigated from first-principles, within the local-density approximation, using the full-potential linearized augmented plane-wave method. The results show that, besides the large Ta($5d$)-O($2p$) hybridization which is a common feature of the ferroelectric perovskites, there is an important hybridization between bismuth and oxygen states. The underlying static potential for the ferroelectric distortion and the primary source for ferroelectricity is investigated by a lattice-dynamics study using the frozen-phonon approach.

I. INTRODUCTION

Ferroelectric materials can display a wide range of dielectric, ferroelectric, piezoelectric, electrostrictive, and pyroelectric properties. The potential utilization of these properties in a new generation of devices has motivated intensive studies. For example, the high dielectric permittivities of perovskite-type materials, like $Sr_xBa_{1-x}TiO_3$, can be advantageously used in dynamic random access memories, while the large values of switchable remanent polarization of ferroelectric materials are suitable for nonvolatile ferroelectric random access memories.[1–4]

The most popular ferroelectric materials for nonvolatile memory applications are $PbZr_xTi_{1-x}O_3$ (PZT), because they have a high Curie temperature and large remanent polarization. However, these materials have serious fatigue degradation problems which can be solved by the modification of the electrode. An alternative approach to controlling the fatigue problem in ferroelectric capacitors is to use other ferroelectric materials. In recent years, $SrBi_2Ta_2O_9$ (SBT) has emerged as an important candidate for nonvolatile ferroelectric memories.[5,6] It exhibits many desirable properties in order to be considered as an important component of the memory devices under development: almost no fatigue after 10^{12} switching cycles, good retention characteristics, low switching fields and low leakage currents.

Bismuth-containing layered perovskites have been found to be ferroelectric by Smolenskii, Isupov, and Agranovskaya.[7] These materials belong to the family of Aurivillius compounds with a general formula $(Bi_2O_2)^{2+}(A_{m-1}B_mO_{3m+1})^{2-}$, consisting of m perovskite units sandwiched between bismuth oxide layers[8] (here A and B are the two types of cations that enter the perovskite unit).

It is well known that the Aurivillius composition $SrBi_2Ta_2O_9$ (SBT) has ferroelectric behavior at room temperature. Its crystal structure was investigated by Rae and co-workers.[9] The room-temperature structure is orthorhombic (space group $A2_1am$) and the primitive cell contains 28 atoms. The lattice parameters of the conventional unit cell are $a=5.531$ Å, $b=5.534$ Å, and $c=24.984$ Å. As a result, its electrical properties are expected to exhibit a high degree of anisotropy. For instance, it was observed that the ferroelectricity along the c axis is absent or very low,[10] with a being the polar axis. More recently, this property was confirmed at the submiscropic level by piezoresponse scanning-force microscopy.[11]

The complex crystal structure of SBT can be described in terms of relatively small perturbations from a high-symmetry body-centered tetragonal structure (space-group symmetry $I4/mmm, a=b\approx 5.53/2^{1/2}=3.91$ Å), which contains only one formula unit per primitive cell (as in other orthorhombic structures, the a and b axes are rotated by 45° with respect to the tetragonal case).

Although the orthorhombic symmetry is responsible for the ferroelectricity in SBT, the parent tetragonal structure shown in Fig. 1 provides a convenient simplification for visualizing and dealing with the complex SBT structure. As a matter of fact, most bismuth layer compounds have been reported to be pseudotetragonal, with tetragonal symmetry above the Curie point and orthorhombic symmetry below it (for SBT the Curie temperature is 608 K). So the parent tetragonal structure of SBT could be related to the crystal structure of its paraelectric phase. Two main distortions from the tetragonal prototype structure lead to the orthorhombic structure. First, the ions displace along the orthorhombic a axis ([110] axis of the tetragonal structure). Second, the TaO_6 octahedra rotate around the a and c axes. The first factor is directly responsible for the observed macroscopic spontaneous polarization along the a direction.

In spite of its technological importance, theoretical studies

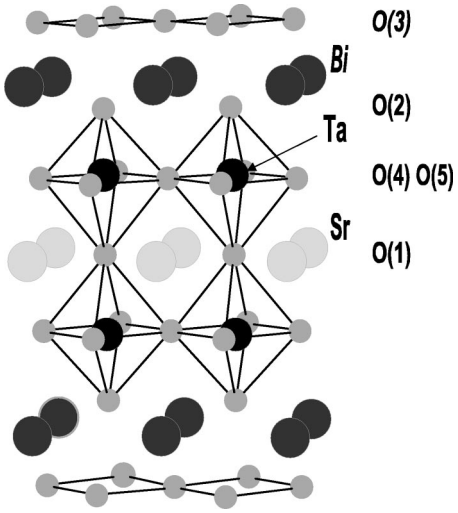

FIG. 1. Tetragonal structure of $SrBi_2Ta_2O_9$. Only atoms between $\frac{1}{4}c$ and $\frac{3}{4}c$ are shown.

on SBT are limited due to the complexity of its crystal structure. The band structure of SBT was initially calculated by Robertson *et al.* using the tight-binding method,[12] where a highly simplified orbital basis set was used to reproduce the main features of the bonding. They used an orthogonal basis of O p, Ta d, and Bi s and p orbitals, and no orbitals on the Sr. The interaction parameters were found by transferring them from established band structures of other compounds. Their results show that both the valence and conduction band extrema are composed of states localized mainly on the Bi-O layer. It was argued that the Bi_2O_2 layer dominates the electronic response (band gap, effective masses, etc.), while the ferroelectric response largely originates from the $SrTa_2O_7$ perovskite blocks.

Several other speculations have been made about the origin of ferroelectricity in SBT and related compounds. Among them are the central role of Sr^{+2} ion diplacements,[13] the off-center position of Ta^{+5} ion relative to its octahedron of surrounding oxygens,[14] and the movement of the Ta-O plane relative to the Bi-O plane.[9]

More recently, the difference between the electronic structures of $SrBi_2Ta_2O_9$ and $SrBi_2Nb_2O_9$ (SBN) was investigated using the discrete variational X-α cluster method.[15] The results indicate that the difference in the remanent polarizations in SBT and SBN is due to the different displacements of Ta and Nb at the B sites of a pseudo-perovskite layer, and not due to differences in the displacement of the other ions. However, one cannot expect high-accuracy results for relaxations and electronic states in crystalline materials from cluster methods. Thus there is a need for the application of highly precise self-consistent band-structure methods.

In this work we present a first-principles study of the electronic structure and ferroelectric instability in SBT. The calculations were performed within the local-density approximation to density-functional theory, using the full-potential linearized augmented plane-wave method.

II. METHOD

The calculations presented in this work were performed using the full-potential linearized augmented plane-wave method (LAPW) method (see, e.g., Ref. 16) with the addition of local-orbital basis functions[17] as implemented in the WIEN97 code.[18] Exchange and correlation effects were treated within the local-density approximation (LDA), using the parametrization by Perdew and Wang.[19]

TABLE I. Equilibrium atomic coordinates in lattice constant units ($a=3.91$ Å and $c=24.984$ Å).

Atom	X	Y	Z
Sr	0.0	0.0	0.0
Ta	0.5	0.5	± 0.08468
Bi	0.0	0.0	± 0.20124
O(1)	0.5	0.5	0.0
O(2)	0.5	0.5	± 0.16033
O(3)	0.0 (0.5)	0.5 (0.0)	0.25
O(4)	0.0	0.5	± 0.07602
O(5)	0.5	0.0	± 0.07602

The muffin-tin sphere radii $R_i=2.0,\ 1.8,\ 2.3$, and 1.5 a.u. were used for Sr, Ta, Bi, and O, respectively. The value of the parameter $RK_{\max}$, which controls the size of the basis set for the wave functions, was chosen to be 7.3 for all the calculations. This resulted in well-converged basis sets consisting of approximately 2500 LAPW functions. For the Sr-4s and 4p, Ta-5s, 5p and 4f, Bi-6s and 5d, and O-2s states local orbitals were chosen in addition. Integrations in reciprocal space were performed using the tetrahedron method. We used a $6\times6\times6$ mesh which represents 28 k points in the irreducible wedge for the body-centered-tetragonal structure. Convergence tests indicate that only small changes result from going to a denser k mesh or to a larger value of $RK_{\max}$.

III. RESULTS AND DISCUSSION

A. Electronic structure

The electronic structure of SBT is calculated for the tetragonal parent structure. We use the experimental lattice constants $a=3.91$ Å and $c=24.984$ Å. Since the internal parameters of this structure have not been determined experimentally, we evaluated the equilibrium positions of the atoms using a damped Newton dynamics method. (The final force on each atom was less than ≈ 1 mRy/a.u.) The equilibrium coordinates are listed in Table I.

The band structure of the optimized geometry is shown in Fig. 2 along several high-symmetry lines in the Brillouin zone. Roughly speaking, the two bands centered at ≈ -10 eV are derived from Bi 6s orbitals while the manifold of 27 valence bands are derived mainly from O 2p orbitals. We found that the fundamental band gap is indirect, since the valence band maximun lies at X while the conduction band minimun is the Brillouin-zone center Γ. As is typical in LDA calculations for semiconductors, the band gap is underestimated. The experimental band gap obtained from UV-absorbance measurements is 4.2 ± 0.2 eV,[20] which is twice as large as our theoretical value of ≈ 2 eV. It is interesting to note that, in disagreement with our results, an indirect (Γ-M) band gap was obtained by the tight-binding calculation,[12] which indicates important differences in the details of the dispersion.

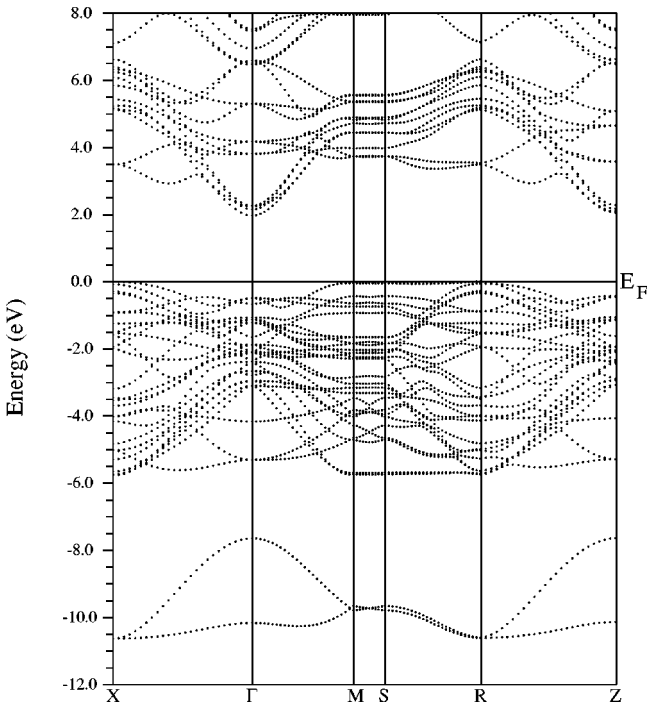

FIG. 2. Band structure of $SrBi_2Ta_2O_9$ along several high-symmetry lines in the Brillouin zone.

The total density of states between -35 and 5 eV is shown in Fig. 3 illustrating the energy position of the semicore states. The calculated total DOS is in reasonable agreement with x-ray photoemission spectroscopy data, which show a valence band width of ≈ 7 eV and a peak centered ≈ 10 eV below the valence band maximum (Bi $6s$ band).[20]

Although the valence band presents mainly O $2p$ character, there is a quite strong hybridization with Bi and Ta states, as is evident from the sphere-projected density of states (DOS) shown in Fig. 4. Examination of the DOS reveals that there is substantial O $2p$ character in the conduction bands, rising from zero at the conduction band minimum with increasing energy. Conversely, there are strong Ta and Bi contributions to the valence band. The Ta $5d$ contribution is zero at the valence band maximum but rises strongly with decreasing binding energy, reflecting the Ta $5d$-O $2p$ covalency (as it is common in ABO_3 perovskites). The Bi contribution has both *s*-like (mainly in the upper part of the valence band) and *p*-like (mainly in the lower part) character.

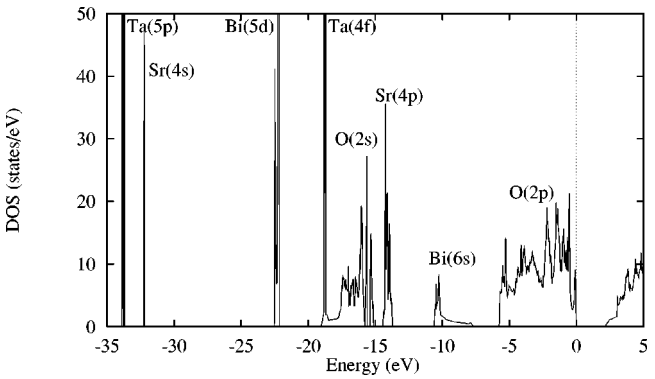

FIG. 3. Total density of states for $SrBi_2Ta_2O_9$, between -35 and 5 eV, showing the energy position of the semicore states.

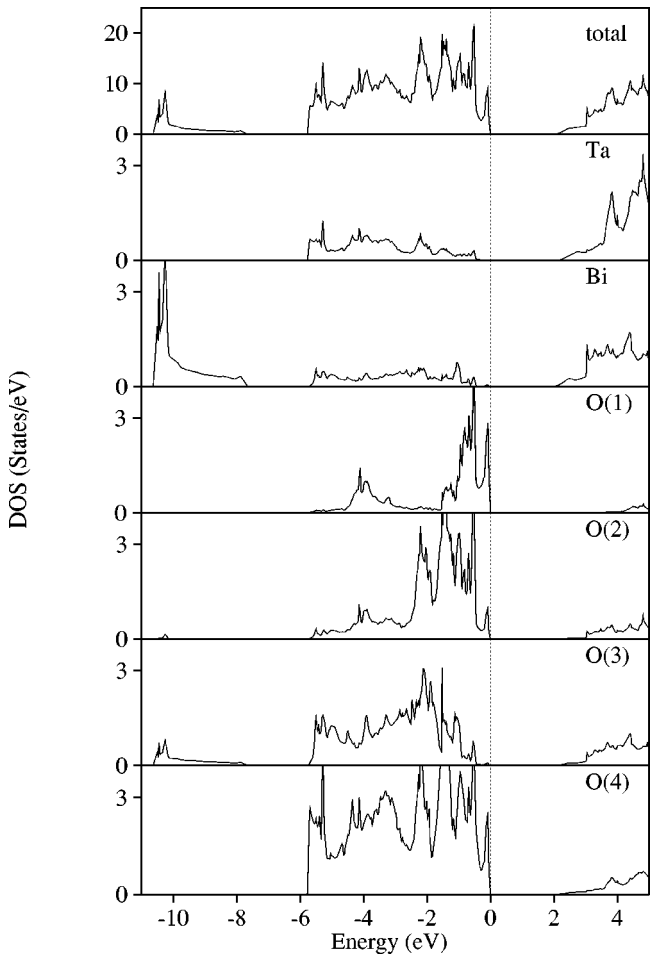

FIG. 4. Total and site-projected electronic densities of states for the valence and conduction bands of $SrBi_2Ta_2O_9$.

These contributions arise from a strong hybridization between O(2,3) $2p$ valence band states with Bi $6s$ (fully occupied) and Bi $6p$ (conduction) bands. A detalied examination of the band characters reveals that the valence band maximum and the conduction band minimum are not mainly localized in the Bi-O(3) layer, as was obtained by the tight-binding calculation.[12] In fact, in our case the valence band maximum at X is primarily of O(1,4) $2p$ character.

We finally show in Fig. 5 the valence charge density map of SBT in two high symmetry planes, where the Ta-O and Bi-O ''covalent bonds'' can be seen.

B. Ferroelectric instability

The main features of SBT described so far resembles the electronic structure of $PbTiO_3$. In this material, besides the large Ti $3d$-O $2p$ hybridization, there is an important hybridization between Pb $6s$ and O $2p$ states; and this covalent bond plays a central role in the stabilization of the tetragonal ferroelectric structure of $PbTiO_3$.[21]

The presence of quite strong Ta-O and Bi-O hybridizations in SBT opens fundamental questions about the origin of its ferroelectricity: What is the underlying static potential for the ferroelectric distortion? Which is the primary source for ferroelectricity? We investigate these questions by a lattice dynamics study using the frozen-phonon approach.

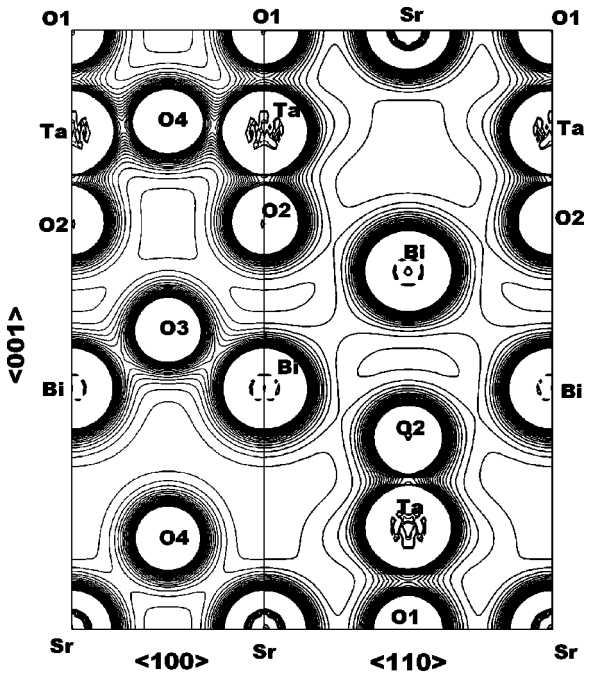

FIG. 5. Valence charge density plot in the (100) and (110) planes of $SrBi_2Ta_2O_9$. The scale is from 0 to 0.2 electrons per $Bohr^3$ and the contour interval is 0.01 electrons/$Bohr^3$.

To search for the presence of a possible lattice instability of the tetragonal structure, we determined the phonon frequencies and eigenvectors of the infrared-active E_μ modes, which are polarized perpendicular to the c axis. To this end, we calculated atomic forces for several small displacements (~ 0.01 Å) consistent with the symmetry of the mode. From the force as a function of displacement, the dynamical matrix was constructed and diagonalized. The calculated frequencies and eigenvectors are listed in Table II.

While experimental studies were carried out on infrared-active (IR) phonons in orthorhombic SBT, using reflectivity and transmission measurements,[22] there is no experimental determination of IR phonon frequencies for the tetragonal structure to directly compare with. The remarkable fact of our calculation is, however, the presence of one unstable phonon mode. The eigenvector of this mode, shown in Table II, indicates that it mainly involves movements of the Bi atoms with respect to rest of the lattice. The displacement vector is obtained from this eigenvector by dividing each component by the square root of the corresponding atomic mass. By normalizing to unity, the displacement pattern is (0.085, 0.114, −0.206, 0.325, 0.549, 0.053, 0.224, 0.182). This pattern shows large displacements of the TaO_6 perovskite-like blocks relative to Bi atoms. So, the polarity of the mode can be described as a vibration of the TaO_6 perovskite-like block relative to Bi, with an additional contribution arising from the movement of Ta relative to its surrounding oxygens. Rae *et al.*[9] argued that the polarity of orthorhombic SBT can be quite well described as a movement of Ta, O(4) and O(5) relative to Bi and O(3) of the BiO_2 layer with and additional movement of Ta relative to O(4) and O(5). Although the displacement pattern of the unstable mode is not directly related with the atomic positions of the orthorhombic phase, both pictures show some consistence. It is worth to mention that, from a detailed analysis of the calculated force constants, the lattice instability primarily arises from the attractive Bi-O(2) interaction.

The resulting in-phase movement of the Ta atoms with respect to their oxygen octahedra (obtained from the eigenvector of the ferroelectric mode), could be the explanation of the low remanent polarization observed in SBT. However, this situation could be different for the case of SBN, considering the different structural behavior of $KNbO_3$ and $KTaO_3$. While $KNbO_3$ has a series of ferroelectric phase transitions, $KTaO_3$ remains cubic down to low temperatures. Furthermore, it was emphasized by Singh,[23] that the absence of ferroelectricity in $KTaO_3$ is due to the extreme sensitivy of the soft-mode to the covalency and the slight chemical differences of Nb and Ta, particularly the higher d binding energy of Nb. This point will be clarified in the future by a corresponding investigation on SBN.

Finally, the total energy is evaluated as a function of the displacement pattern corresponding to the unstable mode. The results are shown in Fig. 6 which depicts the energy per formula unit for displacement patterns along the [100] and [110] direction, respectively. Ferroelectric instabilities with energy gains of ≈ 4 and 6 mRy/cell for the [100] and [110] directions are observed. Although the ferroelectric mode mainly involves displacements of the Bi atoms with respect to rest of the lattice, a [110] displacement of the Bi sublattice alone does not produce a lattice instability (see Fig. 6). This indicates that Bi does not have a tendency to go off-center in the tetragonal phase, and the energy wells presented in the figure are indeed associated with the specific pattern of atomic displacements of the ferroelectric mode.

TABLE II. Frequencies ω and eigenvectors of the E_μ modes, which are polarized perpendicular to the c axis.

ω	Eigenvector							
(cm^{-1})	Sr	Ta+	Bi+	O(1)	O(2)+	O(3)+	O(4)+	O(5)+
495	0.036	0.052	0.001	0.432	0.033	−0.001	−0.617	0.148
247	−0.051	0.064	0.053	−0.754	0.324	−0.205	−0.212	0.125
215	−0.032	0.053	−0.117	−0.360	−0.122	0.621	−0.113	0.073
113	−0.786	0.395	−0.026	0.019	−0.120	−0.066	−0.019	−0.122
100	0.147	0.037	0.031	0.010	0.239	0.108	−0.129	−0.634
73	0.502	0.301	−0.191	−0.232	−0.403	−0.199	−0.088	−0.103
i54	0.130	0.251	−0.489	0.213	0.360	0.035	0.147	0.120

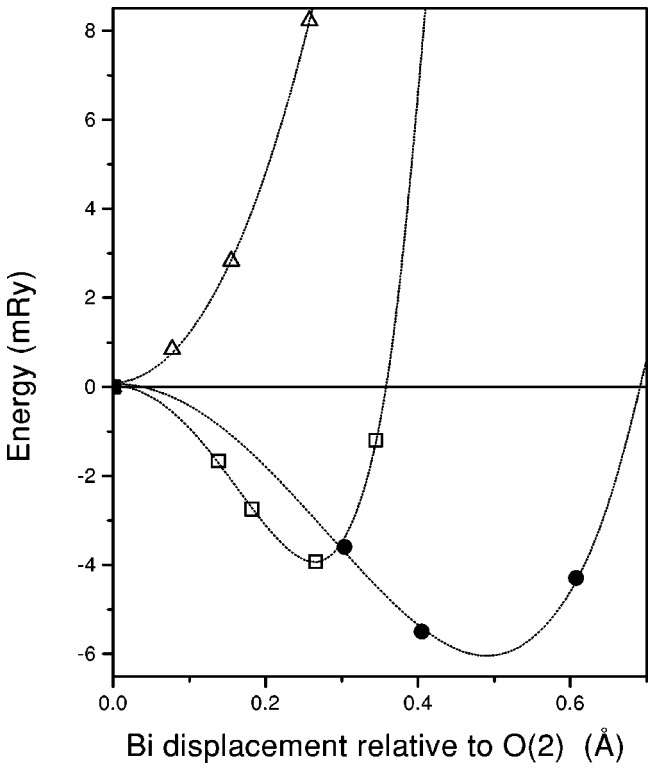

FIG. 6. Energy as a function of the distortion along the [110] (●) and [100] (□) directions corresponding to the unstable mode. The normal coordinate is represented by a motion of Bi relative to O(2). The energies are with respect to that of the perfect tetragonal structure. The energy as a function of the [110] displacement of the Bi sublattice is also shown (△).

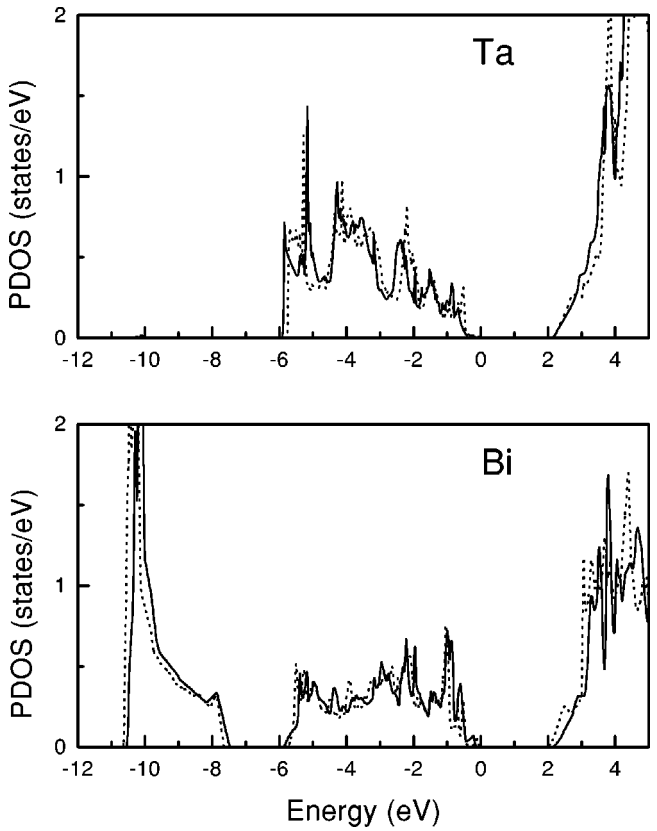

FIG. 7. Comparison of the partial density of states for Ta and Bi in the tetragonal structure, with (full line) and without (dotted line) displacements of the ions, according to the displacement pattern of the unstable mode along the [110] direction.

As already mentioned, the bonding of these materials stems from the transition-metal–oxygen hybridization. As can be seen from Fig. 7, the whole spectrum of eigenvalues gets modified in an intricate way upon the complex distortion that gives rise to the instability. The two main effects are an increase in the band gap and a decrease of the separation between the Bi-*s* states and the valence band. When the distortion sets in, spectral weight from the lower part of the conduction band gets reduced and transfered to higher energies. This is more pronounced in the Bi contribution to the DOS than in that of Ta. In the valence region, the DOS gets reduced at the top and increased at the bottom. Here, the effect on the Ta contribution is stronger. So, both covalent bonds seem to play an important role. It is worth mentioning however, that the energetics shown in Fig. 6 finally comes from a very delicate balance between several contributions: covalent, Coulomb, and repulsive ionic interactions.

The [110] displacement results in a deeper total-energy minimum, which is consistent with the fact that the low-temperature ferroelectric state of SBT has orthorhombic symmetry. The existence of a saddle point in the [100] direction on the total energy surface could indicate that the phase transition in SBT is not as simple as considered until now. In order to discuss this point it is useful to note some aspects of the dynamical mechanism leading to the sequence of phase transitions in ABO_3 perovskites. Theses crystals have been considered for a long time to be displacive-type ferroelectrics. The main evidence for this behavior has been the existence of a Γ-TO soft mode which has been observed in many perovskites.[24,25] However, there is experimental[26–30] as well as theoretical[31–33] evidence that the sucessive phase transitions in $KNbO_3$, and $BaTiO_3$, have pronounced order-disorder features, and that they are quite well described in the framework of the eight-site model. According to this order-disorder approach, the total-energy surface has a maximum for the cubic perovskite structure, eight degenerate minima for the [111] soft mode amplitude displacements, and saddle points for the [100] and [110] displacements. In the cubic phase, the eight minima are occupied with equal probability, where this symmetry is broken as the temperature is lowered: Four sites are occupied in the tetragonal phase, two sites in the orthorhombic phase, and finally, only one site is occupied in the rhombohedral structure. In this way, the relaxation process which displays a critical slowing down when T_c is approached in the different phases is interpreted to be the driving mechanism of the phase transitions.

The lattice instability related to the ferroelectric phase transition of SBT was recently studied by Raman scattering in the temperature range between 293 and 958 K.[34] The lowest frequency mode of 29 cm^{-1} at room temperature showed remarkable temperature variations towards T_c. While its frequency decreases markedly, the damping factor increases rapidly below T_c. This fact may suggest that the nature of the phase transition shows a crossing over from displacive to order-disorder type in the neighborhood of T_c. As in $KNbO_3$, it was also found, that the extrapolated frequency is still finite at T_c, where this relatively large value

may originate not only from the first-order phase transition, but also due to the coupling between the soft mode and the strain.

If this coupling between soft mode and strain is strong enough, the energetics shown in Fig. 6 would give rise to the presence of an intermediate phase in SBT, leading to the following phase-transition sequence: paraelectric (tetragonal) → ferroelectric (net polarization along the [100] direction → ferroelectric (orthorhombic, net polarization along the [110] direction). As in the eight-site model, the four energy minima would be occupied with equal probability in the high-temperature paraelectric phase, two sites would be occupied in the intermediate phase (with a net polarization along the [100] direction), and finally, one site would be occupied in the orthorhombic phase.

Recently, an anomaly at $T=520$ K was observed in specific-heat measurements of SBT films.[35] For Bi-rich $Sr_{0.8}Bi_{2.2}Ta_2O_9$ two anomalies were found at 620 and 410 K, with corresponding changes in the x-ray-diffraction pattern suggesting structural changes. The introduction of a small amount of excess Bi improved significantly the ferroelectric properties of SBT [the spontaneous polarization is two times larger and the Curie temperature shift to 670 K from 608 K (Ref. 36)]. These results also suggest that the phase transition in SBT is not as simple as considered until now. More detailed examinations of crystal symmetry and dielectric measurements on single crystals are necessary for clarifying the nature of ferroelectricity in the SBT family compounds.

ACKNOWLEDGMENTS

M.G.S. thanks CONICET, CIUNR, and FONCyT for support. C.A.D. acknowledges support from the Austrian Science Fund, Project No. P13430-PHY.

[1] M.C. Scott and C.A. Paz de Araujo, Science **246**, 1400 (1989).
[2] J.F. Scott, Phys. World **46**, No. 2 (1995).
[3] O. Auciello, J.F. Scott, and R. Ramesh, Phys. Today **51** (7), 22 (1998).
[4] J.F. Scott, Ferroelectrics **1**, 1 (1998).
[5] S.B. Desu and D.P. Vijay, Mater. Sci. Eng., B **32**, 75 (1995).
[6] C.A. Paz de Araujo, J.D. Cuchiaro, L.D. McMillan, M.C. Scott, and J.F. Scott, Nature (London) **374**, 627 (1995).
[7] G.A. Smolenskii, V.A. Isupov, and A.I. Aganoskaya, Fiz. Tverd. Tela Leningrad **3**, 477, (1961) [Sov. Phys. Solid State **3**, 651 (1961)].
[8] B. Aurivillius, Ark. Kemi **1**, 463 (1949).
[9] A.D. Rae, J.G. Thompson, and R.L. Withers, Acta Crystallogr., Sect. B: Struct. Crystallogr. Cryst. Chem. **48**, 418 (1992).
[10] S.B. Desu, D.P. Vijay, and B. He, Appl. Phys. Lett. **69**, 1719 (1996).
[11] A. Pignolet, K. Satyalakshmi, M. Alexe, N. Zakharov, C. Harnagea, S. Senz, D. Hesse, and U. Gösele (unpublished).
[12] J. Robertson, W. Chen, W.L. Warren, and C.D. Gutleben, Appl. Phys. Lett. **69**, 1704 (1996).
[13] J. Lui, G. Zou, H. Yang, and Q. Cui, Solid State Commun. **90**, 365 (1994).
[14] R.E. Newnham, R.W. Wolfe, R.S. Horsey, F.A. Diaz-Colon, and M.I. Kay, Mater. Res. Bull. **8**, 1183 (1973).
[15] K. Miura and M. Takana, Jpn. J. Appl. Phys., Part 1 **37**, 606 (1998).
[16] D. J.Singh, *Planewaves, Pseudopotentials and the LAPW Method* (Kluwer Academic, Boston, 1994).
[17] D.J. Singh, Phys. Rev. B **43**, 6388 (1991).
[18] P. Blaha, K. Schwarz, and J. Luitz, *WIEN97*, A Full Potential Linearized Augmented Plane Wave Package for Calculating Crystal Properties, Karlheinz Schwarz, Techn. Universität Wien, Austria, 1999, ISBN 3-9501031-0-4.
[19] J.P. Perdew and Y. Wang, Phys. Rev. B **45**, 13 244 (1992).
[20] A.J. Hartmann, R.N. Lamb, J.F. Scott, and C.D. Gutleben, Integr. Ferroelectr. **18**, 101 (1997).
[21] R.E. Cohen, Nature (London) **358**, 136 (1992).
[22] M.P. Moret, R. Zallen, R.E. Newnham, P.C. Joshi, and S.B. Desu, Phys. Rev. B **57**, 5715 (1998).
[23] D.J. Singh, Phys. Rev. B **53**, 176 (1996).
[24] W. Cochram, Adv. Phys. **9**, 387 (1960).
[25] J.F. Scott, Rev. Mod. Phys. **46**, 83 (1974).
[26] M.D. Fontana, G. Métrat, J. Servoin, and F. Gervais, J. Phys. C **16**, 483 (1984).
[27] H. Vogt, M.D. Fontana, G.E. Kugel, and P. Günter, Phys. Rev. B **34**, 410 (1986).
[28] M.D. Fontana, G. Ridah, G.E. Kugel, and C. Carabatos-Nedelec, J. Phys. C **21**, 5853 (1988).
[29] J.P. Sokoloff, L.L. Chase, and D. Rytz, Phys. Rev. B **38**, 597 (1988).
[30] A.I. Frenkel, F.M. Wang, S. Kelly, R. Ingalls, D. Haskel, E.A. Stern, and Y. Yacoby, Phys. Rev. B **56**, 10 869 (1997).
[31] A. Postnikov, T. Neumann, G. Borstel, and M. Methfessel, Phys. Rev. B **48**, 5910 (1993).
[32] M. Sepliarsky, M.G. Stachiotti, and R.L. Migoni, Phys. Rev. B **56**, 566 (1997).
[33] M.G. Stachiotti, M. Sepliarsky, R.L. Migoni, and C.O. Rodriguez, in *First-Principles Calculations for Ferroelectrics*, edited by R.E. Cohen, AIP Conf. Proc. No. 436 (AIP, Woodbury, 1998), p. 274.
[34] S. Kojima, J. Phys.: Condens. Matter **10**, L327 (1998).
[35] A. Onodera, K. Yoshio, C. C. Myint, M. Tanaka, K. Hironaka, and S. Kojima (unpublished).
[36] K. Takemura, T. Noguchi, T. Hase, and Y. Miyasaka, Appl. Phys. Lett. **73**, 1649 (1998).